RETRACTION
https://doi.org/10.1071/CH18268_RE

AUSTRALIAN JOURNAL OF CHEMISTRY

Retraction notice to 'A Biocompatible Gd^{III}-Organic Framework Incorporating Polar Pores for pH-Sensitive Anti-Cancer Drug Delivery and Inhibiting Human Bone Tumour Cells'

Mingliang Ren, Hui Li, Hu Liu, Lei Wang, Haibo Xiang, Xianrong Zhang and Bin Yu

Refers to: RETRACTED: A Biocompatible Gd^{III}-Organic Framework Incorporating Polar Pores for pH-Sensitive Anti-Cancer Drug Delivery and Inhibiting Human Bone Tumour Cells, published 17 December 2018, https://doi.org/10.1071/CH18268. Mingliang Ren, Hui Li, Hu Liu, Lei Wang, Haibo Xiang, Xianrong Zhang and Bin Yu.

After due consideration of issues raised with respect to this paper, the Editors-in-Chief and the authors agree to retract the paper from *Australian Journal of Chemistry*.

Reason: Upon review of the submission history for the manuscript, the *Australian Journal of Chemistry* Editors and Publisher found indications that the peer review process is likely to have been compromised by the submission of reviews through suspected fabricated reviewer accounts.

The Editors-in-Chief and Journal Publisher have determined these are grounds for retraction, according to the international guidelines established by the Committee on Publication Ethics. We regret the academic record was compromised and apologise for any inconvenience this may have caused.

Ren M *et al.* (2023) *Australian Journal of Chemistry*
76(2), 115. doi:10.1071/CH18268_RE

CSIRO PUBLISHING

Aust. J. Chem.
https://doi.org/10.1071/CH18268

Full Paper

A Biocompatible Gd^{III}–Organic Framework Incorporating Polar Pores for pH-Sensitive Anti-Cancer Drug Delivery and Inhibiting Human Bone Tumour Cells

Mingliang Ren,[A,B,C] *Hui Li,*[C] *Hu Liu,*[C] *Lei Wang,*[A,B] *Haibo Xiang,*[A,B] *Xianrong Zhang,*[A,B] *and Bin Yu*[A,B,D]

[A]Department of Orthopaedics and Traumatology, Nanfang Hospital, Southern Medical University, Guangzhou 510515, China.
[B]Key Laboratory for Bone and Cartilage Regeneration, Nanfang Hospital, Southern Medical University, Guangzhou 510515, China.
[C]Department of Orthopaedics, Affiliated Nanhai Hospital, Southern Medical University, Foshan 528200, China.
[D]Corresponding author. Email: bin_yu666@126.com

With the aim of developing new and effective drug delivery systems for cancer treatments, great effort has been devoted to the field of porous metal–organic framework (MOF) platforms because of their controlled drug release performance, high drug loading, and acceptable biocompatibility. In this contribution, we report a MOF $[Gd_2(H_2O)_3(SDBA)_3](DMA)_3]$ (**1**, DMA = *N*,*N*-dimethylacetamide) with open O donor sites functionalised 1D pores, which has been fabricated using a bent polycarboxylic acid organic linker 4,4′-sulfonyldibenzoic acid (H_2SDBA) under solvothermal conditions. Single crystal X-ray diffraction (SCRD), thermogravimetric analysis (TGA), elemental analysis, X-ray powder diffraction (XPRD), and Brunauer–Emmett–Teller (BET) analysis were used to characterise the as-prepared complex **1**. 5-Fluorouracil (5-Fu) loaded **1** was soaked in phosphate buffer saline (PBS) and the in vitro drug release performance was monitored by HPLC analysis under different pH conditions. At the pH values of 7.4 and 6.5, different profiles of pH-responsive release were achieved, indicating that the drug release performance of 5-Fu loaded **1** is pH sensitive. Grand Canonical Monte Carlo (GCMC) simulation results demonstrate that the open O donor sites in the framework of **1** account for the slower drug release rate. The prepared carrier is found to be bio-compatible with MG63 cells (cancerous tissue) and oral epithelial cells (normal tissue), when tested by 3-(4,5-dimethylthiazol-2-yl)-2,5-diphenyltetrazolium bromide (MTT) assay. The 5-Fu loaded carrier also shows a promising growth inhibition effect towards the human bone tumour cells MG63.

Manuscript received: 2 June 2018.
Manuscript accepted: 23 November 2018.
Published online: 7 December 2018.

Introduction

Although great progress has been achieved in the field of biomedicine, cancer is still one of the most life-threatening diseases that kills millions of people every year.[1] Since the clinical success of anticancer drugs such as cisplatin and its analogues, chemotherapy that depends on anticancer drugs has become the dominant therapy method for most cancers.[2] However, the traditional direct administration of cancer drugs to patients has caused some undesirable side effects such as high toxicity to human normal cells, non-selective drug distribution, and low drug stability, which may damage healthy tissues and limit the therapeutic effect.[3] Furthermore, many tumours are highly resistant to conventional anticancer drugs, which require that the anticancer drugs need to accumulate in tumour regions with a high enough concentration to kill the cancer cells.[4] To address the above mentioned issues, nanoporous drug delivery systems (NDDS) that utilise various porous carriers to load drugs have gained much attention in recent years because they not only had a large loading capacity for the targeted drug molecules but could also release many more drug molecules in tumour tissue than they do in normal tissues, resulting in a high drug concentration in the cancerous tissue. In the past few decades, many types of porous materials such as carbon nanotubes, porous silica particles, and polymeric micelles, have been studied and applied as drug carriers, but they still suffer from some drawbacks such as low drug loading capacity and poor biocompatibility.[5–7]

As a burgeoning class of crystalline porous materials, metal–organic frameworks (MOFs) made of metal ion/clusters as nodes and polydentate organic ligands as connectors have been of great research interest in the last two decades not only for their beautiful structures, but also because of their open active sites, well defined pore structure, and large inner spaces, which are conducive to incorporate targeted guest molecules in the pores.[8–10] The endless possibility in the selection of organic ligands and inorganic ions/clusters make MOFs an adjustable porous material for various targeted applications including

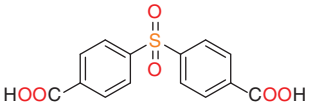

Fig. 1. Molecular structure of the H_2SDBA ligand.

fluorescent sensing, heterogeneous catalysis, gas separation, and biomedicine.[8–16] In particular, porous MOFs have been widely studied as candidates for anticancer drug delivery, exhibiting various superior properties such as high drug loading capacity, suitable pore size, and strong framework–drug interactions.[17–28] Furthermore, it has been reported that many MOFs could be stable in neutral conditions but partly decompose when the pH value lowers.[29] Considering that cancerous tissue is more acidic than normal issue, it could be anticipated that an MOF-based anticancer drug carrier could rapidly release drugs in cancerous tissue and retard the drug leaking into normal tissue.[30–32] In this contribution, with the aim of developing new and effective drug delivery systems for cancer treatments, great effort has been devoted into the field of porous MOF platforms because of their controlled drug release performance, high drug loading, and acceptable biocompatibility. In this contribution, we report a MOF $[Gd_2(H_2O)_3(SDBA)_3](DMA)_3]$ (**1**, DMA = *N*, *N*-dimethylacetamide) with open O donor sites functionalised 1D pores, which has been fabricated using a bent polycarboxylic acid organic linker 4,4′-sulfonyldibenzoic acid (H_2SDBA, Fig. 1) under solvothermal conditions. Single crystal X-ray diffraction (SCRD), thermogravimetric analysis (TGA), elemental analysis, X-ray powder diffraction (XPRD), and Brunauer–Emmett–Teller (BET) analysis were used to characterise the as-prepared complex **1**. 5-Fluorouracil (5-Fu) loaded **1** was soaked in phosphate buffer saline (PBS) and the in vitro drug release performance was monitored by HPLC analysis under different pH conditions. At the pH values of 7.4 and 6.5, different profiles of pH-responsive release were observed indicating the drug release performance of 5-Fu loaded **1** (5-Fu@**1a**) is pH sensitive. Grand Canonical Monte Carlo (GCMC) simulation results demonstrate that the open O donor sites in the framework of **1** account for the slower drug release rate. The prepared carrier is also biocompatible with MCF-7 cells (cancerous tissue) and oral epidermal cells (normal tissue), when tested by 3-(4,5-dimethylthiazol-2-yl)-2,5-diphenyltetrazolium bromide (MTT) assay. In addition, the 5-Fu loaded carrier shows a promising growth inhibition effect towards the human bone tumour cells MG-63.

Experimental

Chemicals and Instruments

All the chemicals were purchased from commercial sources and used without further purification. The H_2SDBA ligand was obtained from the Shanghai Absin Bioscience reagent company. A dual-beam UV-vis spectrophotometer (TU-1900, BPGI, China) was used to acquire the UV-vis absorption spectra. XRPD data were collected on a Rigaku RU200 diffractometer with Cu K_α radiation. C, H, and N elemental analysis was performed with a Thermo Scientific Flash 2000 analyser. TGA curves were obtained in a N_2 atmosphere in the temperature range of 25–800°C on a TGA/DSC-1 thermogravimetric analyser. HPLC was performed on an Agilent 1200 chromatographic system. The 77 K N_2 isotherm was measured with an automated micropore gas analyser (Autosorb-1) with liquid N_2 as the temperature controller.

Table 1. Crystal data and structure refinements for compound 1

Parameter	1
Chemical formula	$C_{40}H_{43}Gd_2N_3O_{15}S_2$
Formula weight	1184.41
Temperature [K]	293(2)
Crystal system	monoclinic
Space group	$P2_1/c$
a [Å]	18.3268(3)
b [Å]	21.1896(4)
c [Å]	16.0653(3)
α [deg.]	90
β [deg.]	110.927(2)
γ [deg.]	90
Volume [Å^3]	[illegible](2)
Z	[illegible]
ρ_{calc} [g cm^{-3}]	1.7[illegible]
μ [mm^{-1}]	2.4[illegible]0
2θ range for data collection [deg.]	4[illegible] to 49.976
Reflections collected	20172
Independent reflections	8742 [R_{int} 0.0264, R_{sigma} 0.0401]
Data/restraints/parameters	8742/77/777
Goodness-of-fit on [illegible]	1.045
Final R indexes [$>$ [illegible]0]	R_1 0.0319, wR_2 0.0687
Final R indexes [all data]	R_1 0.0418, wR_2 0.0744
Largest diff. peak/hole [e Å[illegible]	1.72/−1.00
CCDC	1865596

Preparation of $[Gd_2(H_2O)_3(SDBA)_3](DMA)_3]$

In a [illegible] mL breaker was placed $Gd(NO_3)_3{\cdot}6H_2O$ (45 mg, 0.1 mmol), H_2SDBA (31 mg, 0.1 mmol), DMA (6 mL), and H_2O (1.5 mL). After the addition of 0.2 mL of HCl (2 M, aq), the solution was vigorously stirred for 30 min at room temperature to obtain a clear solution. The clear solution was transferred into a 20 mL vial and heated at 90°C for 72 h. Yellow sheet-like crystalline products of **1** were obtained by removing the solvent, the products were washed with H_2O and left in the air for one day to dry. Yield 52 % on the basis of the H_2SDBA ligand. Anal. Calc. for $C_{40}H_{43}Gd_2N_3O_{15}S_2$ (1184.4): C 40.56, H 3.66, N 3.55; Found: C 40.28, H 3.98, N 3.45 %.

X-Ray Crystallography

The room-temperature singe crystal XRD measurement was performed on a Bruker Apex II CCD diffractometer with Mo Kα radiation. The structure was solved with the *Superflip* structure solution program and then refined by least-squares minimisation with the *ShellXL* refinement package. All non-hydrogen atoms were refined using anisotropic thermal parameters and all hydrogen atoms were placed in their ideal positions using the AFIX commands. Crystallographic data are summarised in Table 1.

5-Fu Loading and Release

Into 5 mL of MeOH was added 20 mg of 5-Fu, and then the solution was made clear via ultrasonic treatment, followed by addition of 10 mg of synthesised **1a** (the crystalline products of **1** were immersed in MeOH for 72 h to completely remove the lattice DMA molecules, and then heated at 60°C for 12 h under dynamic vacuum to afford the compound **1a**). The prepared suspension was then sealed and stirred (650 rpm) for 24 h at room temperature. The 5-Fu loaded **1a** (5-Fu@**1a**) particles

were filtered under vacuum with a 0.2 μm cellulose acetate (Whatman CA) membrane filter. The loaded particles were dried overnight. The unloaded drug concentration in clear supernatant was then quantified by UV-vis spectrophotometry at $\lambda_{max} = 265$ nm in triplicate. The 5-Fu release from the 5-Fu loaded MOF was measured in PBS at 37°C with two different pH values (7.4 and 6.5). The 5-Fu loaded crystals were soaked in PBS (50 mL). At certain intervals, the resulting solution (0.5 mL) was removed and fresh PBS was added to replace it. The 5-Fu content was then probed using the HPLC analysis.

MTT Assay

The cytotoxicity of 5-Fu, **1**, and 5-Fu@**1a** was investigated against MG63 cells (cancer cells) and oral epidermal cells (normal cells) via the strand MTT assay. For these experiments, the cells were incubated in Dulbecco's Modified Eagle's Medium (DMEM, Neuronbc) with 1 % penicillin/streptomycin (P/S, Boster) and 10 % fetal bovine serum (FBS, pH 7.4) for 24 h. After 24 h cell incubation in the humidified incubator (5 % CO_2), the culture medium was replaced by fresh DMEM containing crystals of **1** or 5-Fu@**1a** with different concentrations (10, 20, 40, and 80 μg mL^{-1}) and incubated with the cells for another 4 h in the incubator. After 48 h of incubation, 10 μL of MTT solution (5 mg mL^{-1}) was added. After 4 h, the culture medium was removed and 150 μL of DMSO was added into each well to dissolve the purple insoluble formazan crystals. Absorbance values of samples were determined with a microplate reader at $\lambda = 490$ nm. Each experiment was carried out three times and averaged.

Results and Discussion

Molecular Structure and Physical Characterisation of 1

An SCRD analysis reveals that complex **1** belongs to the monoclinic space group of $P2_1/c$ and its molecular unit is composed of two crystallographically independent Gd^{III} ions, three fully deprotonated $SDBA^{2-}$ ligands, three coordinated water, and three lattice DMA molecules, which all contribute to a neutral network structure with the chemical formula of $[Gd_2(H_2O)_3(SDBA)_3](DMA)_3$]. As shown in Fig. 2a, different coordination surroundings could be observed for the two Gd^{III} ions (Gd1 and Gd2). Gd1 is eight-coordinated and resides in a distorted triangular dodecahedral coordination environment defined by one O atom from the coordinated water and seven oxygen atoms from five different $SDBA^{2-}$ ligands, which shows a *D*[illegible] symmetry according to the software *SHAPE*; Gd2 also reveals a nine-coordinated mode with a biaugmented trigonal prism geometry, which is defined by six carboxylic oxygen atoms from four different $SDBA^{2-}$ ligands and two coordinated water molecules. The Gd^{III}–O bond distances are in the range of 2.252(3) to 2.526(2) Å, which are comparable with those observed in other Gd^{III}-based coordination polymers.[33–35] Gd1, Gd2, and their symmetry related atoms are held together via the *syn*-bridging carboxylic groups along the *a* axis to afford the 1D secondary building unit (SBU) chains with a Gd1–Gd2 separation of 5.07 Å. As depicted in Fig. 2b, the three $SDBA^{2-}$ ligands show three different types of coordination modes: the type-I $SDBA^{2-}$ ligand is involved in the μ_2-η^1: η^1 and μ_2-η^2: η^1 modes of coordination bridging four Gd^{III} ions; the type-II $SDBA^{2-}$ ligand is involved in the μ_2-η^1: η^1 mode of coordination bridging four Gd^{III} ions; the type-III $SDBA^{2-}$ ligand shows μ_2-η^1: η^1 and μ_1-η^1: η^1 modes of coordination connecting with three Gd^{III} ions. The $SDBA^{2-}$ ligands are bent with C–S–C bond angles ranging from 101.7° to 103.6°, which connect with the 1D SUB channels to give rise to the three-dimensional network with rhombus pores (Fig. 2c). The channels are filled with uncoordinated O donor sites and water occupied Gd^{III} sites, which are activated sites for binding with the guests. The total accessible volume of **1** after removal of the guest and coordinated water molecules is estimated to be 38.7 % using the PLATON/VOID routine. In the framework of **1**, the three $SDBA^{2-}$ ligands in the molecular unit could be judged as 3, 4, and 5-connected nodes and the two Gd^{III} centres can be considered as 5 and 6-connected nodes, so the whole framework of **1** can be abstracted as a 3,4,4,5,6-connected topological network with the Schläfli symbol of {4.6.8}{4^2.6^3.8^5}{4^3.6^2.8}{4^3.6^3}{4^9.6^6}, which has not been included in the TOPOS database (Fig. 2d).

The thermal stability of **1** was evaluated by TGA from room temperature to 800°C (Fig. 3a). Successive weight losses of 20.5 % from 25 to 295°C could be discerned from the TGA curve of complex **1**, corresponding to the release of two coordinated H_2O molecules and three lattice DMA molecules in the pores (calcd: 20.2 %). After a relatively steady plateau until 340°C, a sharp weight loss could be observed, indicating the collapse of the framework of **1**. The PXRD profiles reveal a good match between the simulated curve from the crystal data and the experimental one, indicating that the structures of the as-prepared crystalline products are consist with the crystal structure (Fig. 3b). In view of the following drug delivery experiments, the framework integrity of **1** in PBS solution has been studied by soaking the crystalline samples of **1** in PBS (pH 7.4) for one day at 37°C in an oven, and then collecting the corresponding PXRD patterns. The PXRD results indicate that the framework integrity of complex **1** was maintained in PBS, and this also lays the foundation of complex **1** as a drug carrier in simulated human body conditions. In addition, compound **1** shows pH-dependent framework stability as revealed from the PXRD measurements, which also indicates that the drug release performance of the drug loaded **1** might be pH sensitive. The solvent-free samples of **1** (denoted as **1a** hereafter) were prepared by soaking crystalline samples of **1** in MeOH for 72 h to completely remove the lattice DMA molecules, and were then activated at 60°C for 12 h under high vacuum. The TGA curve of **1a** reveals no obvious weight loss in the temperature range of 25 to 329°C, which confirms that all the lattice guest solvents and the coordinated water molecules have been removed. To establish the permanent porosity of **1a**, BET analysis was carried out by measuring the adsorption isotherms of N_2 at 77 K. As shown in Fig. 3c, the N_2 adsorption isotherm at 77 K reveals a reversible type-I adsorption behaviour with a saturated uptake of 268 cm^3 g^{-1} without any hysteresis, which is characteristic of porous materials with microporous channels. Based on the 77 K sorption isotherm, the calculated Langmuir surface area is 777 m^2 g^{-1} and the BET surface area is 576 m^2 g^{-1}. A density functional theory based model fitted to the adsorption branch of the 77 K N_2 isotherm shows the majority of the pores are around 7.2 Å in size, consistent with the values estimated from the single-crystal structure determination (Fig. 3d).

Drug Delivery Experiments

Considering its polar atom functionalised channels and the large solvent accessible voids, activated **1** (**1a**) might be suitable for loading small guest molecules. 5-Fu, which is a widely used anticancer drug for the treatment of various cancer tumours, was

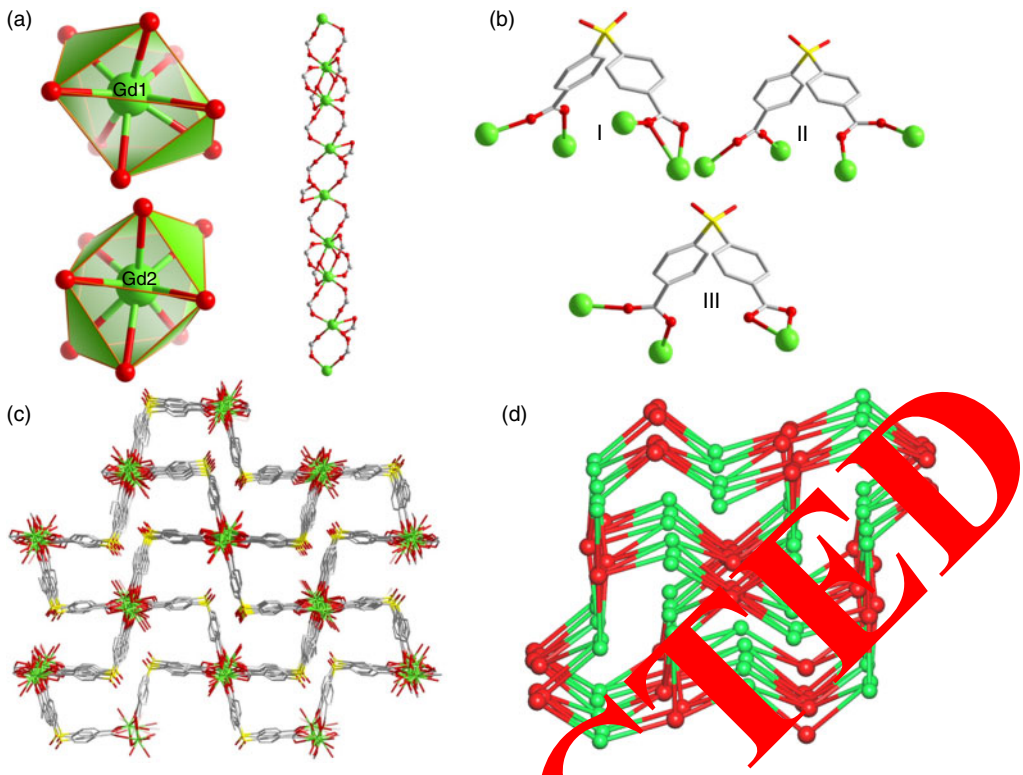

Fig. 2. (a) The coordination surroundings of the Gd^{III} ions and the 1[illegible]BU chain in **1**. (b) The coordination modes for the $SDBA^{2-}$ ligands. (c) The 3D network of **1** showing the rhombus pores. [illegible]The 3,4,4[illegible],6-connected net of **1**.

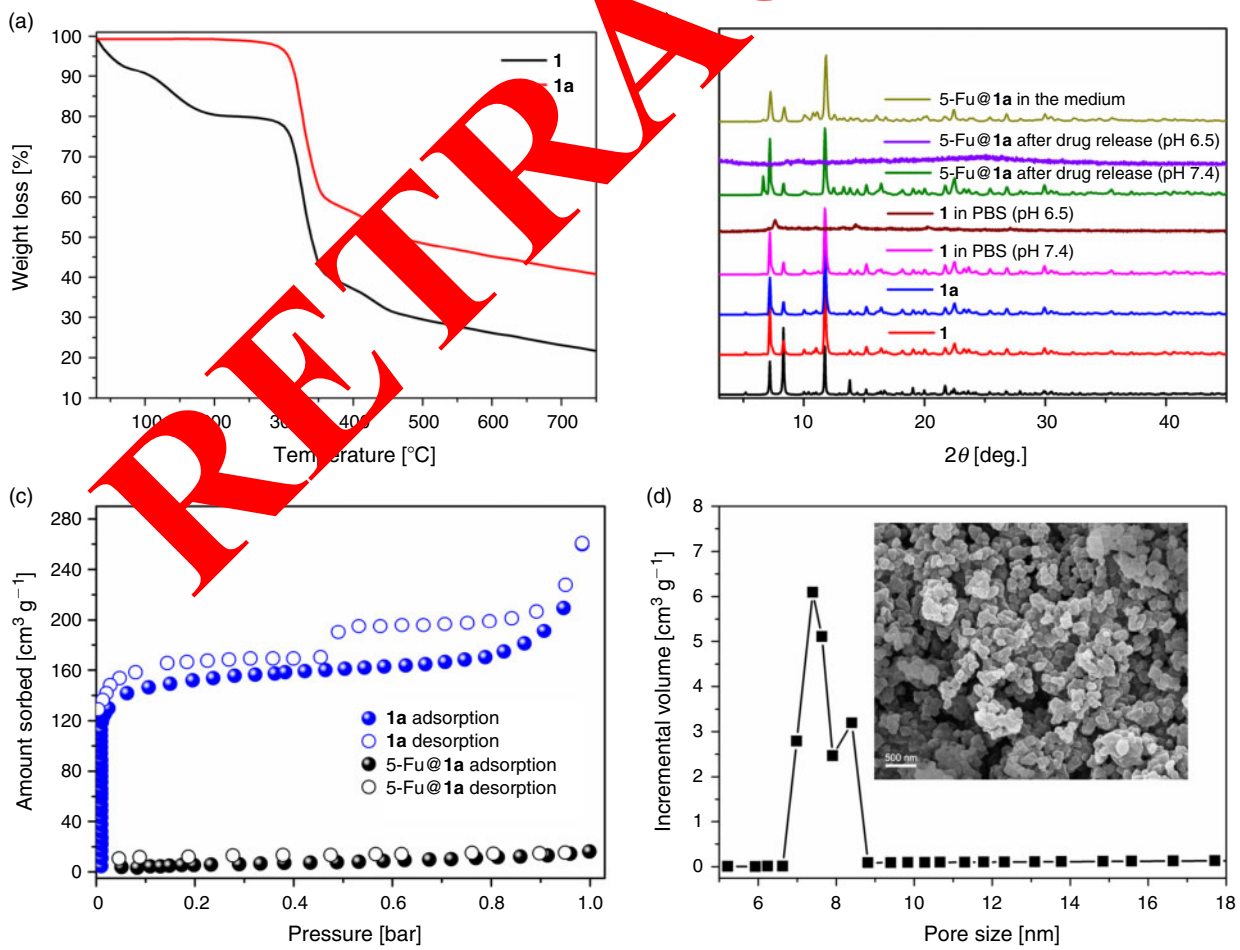

Fig. 3. (a) The TGA profiles for **1** and **1a**. (b) The PXRD profiles for **1**. (c) The N_2 sorption isotherms for **1** and **1a**. (d) The pore size distribution of **1a** (the inset shows the particles size of 5-Fu@**1a** from the SEM image).

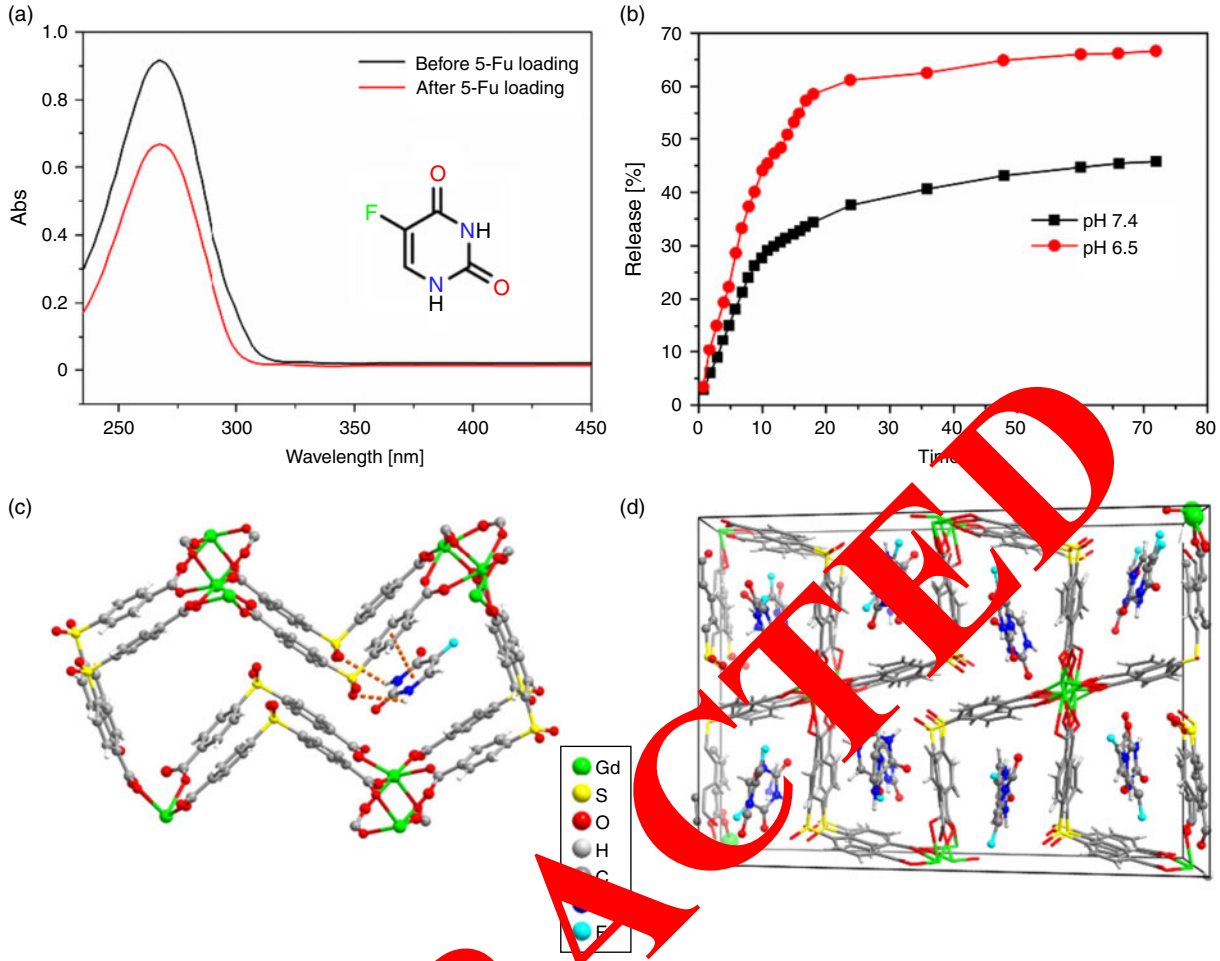

Fig. 4. (a) UV-Vis spectroscopy showing the intensity change before and after 5-Fu loading. (b) Release processes of 5-Fu loaded **1a** under different pH values (7.4 and 6.5). (c) The calculated favourable position of 5-Fu. (d) The calculated distribution of 5-Fu in the framework of **1a**.

chosen as the guest molecule in the framework because of its small molecular size (5.3 × 5.0 Å^2) and the existence of H-bonding donors. In a typical drug loading experiment, the complex **1a** (10 mg) was soaked in 5 mL of MeOH containing 20 mg of 5-Fu with stirring for two hours, and then the drug loading (DL) and encapsulation efficiency (EE) were investigated by UV-vis spectroscopy. Fig. 4a shows the change of the UV-vis spectrum before and after the addition of complex **1a** at 265 nm, the obvious decreased intensity indicates that the 5-Fu molecules in the solution are absorbed into the pores of **1a** (Fig. 4a). Based on the UV-vis spectrum result, the 5-Fu storage capacity is calculated to be 20.6 wt%. Furthermore, the BET analysis via the N_2 sorption experiment at 77 K reveals that the 5-Fu@**1a** shows negligible N_2 uptake capacity (less than 15 cm^3 g^{-1}), reflecting that the pore spaces or the pore windows of **1a** are filled with the 5-Fu molecules. The particle sizes of the resulting products are both around 480 nm as characterised by scanning electron microscopy (SEM), which indicates that the 5-Fu@**1a** could reach specific cancer cells due to its small size (Fig. 3d, inset).

To obtain the 5-Fu drug release profiles of the drug-loaded **1a**, the drug release experiments were performed by dialysing the drug loaded MOF and the concentration of 5-Fu released was determined by HPLC. Fig. 4b shows the drug release profiles at 37°C under two different pH conditions. At pH 7.4, the delivery of 5-Fu occurred within 20 h with no 'burst effect' and no more 5-Fu could be released from the drug loaded MOF with increasing time. This also indicates that the strong drug–framework interaction prevents the drug molecules from escaping from the framework. As mentioned above, the framework of complex **1** shows pH-dependent stability, so the pH value of the PBS solution was adjusted to a more acidic condition (pH 6.5) and the drug release profile was recorded. As expected, the slightly acid condition resulted in a faster 5-Fu release rate with more 5-Fu molecules released into the solution (68 %), demonstrating that the lower pH value can trigger the system of 5-Fu molecule release. The diffraction peaks of 5-Fu@**1a** became broad and did not match with those of **1a**, indicating that the framework of **1a** might partly collapse after drug release at pH 6.5 (Fig. 3b). This feature is beneficial because the drug carrier needs to be degraded after drug release to be eliminated from the human body. To gain a deeper structure–property relationship, we carried out a GCMC simulation to determine the roles of the polar O donor sites in the framework of **1**. The simulated results are shown in Fig. 4c, d. At zero loading and room temperature, one 5-Fu molecule prefers to locate in the channel centre and weak H-bond interactions could be observed (S1–O5···H distance: 2.991 Å and S3–O17···H distance: 2.915 Å). Furthermore, besides the H-bond interactions, there also exist π–π interactions between the 5-Fu molecule and the benzene ring of the ligand with a distance of 3.370 Å. Both the H-bonding and π–π interactions contribute to the strong framework–drug molecule interactions, which prevent the leakage of drug

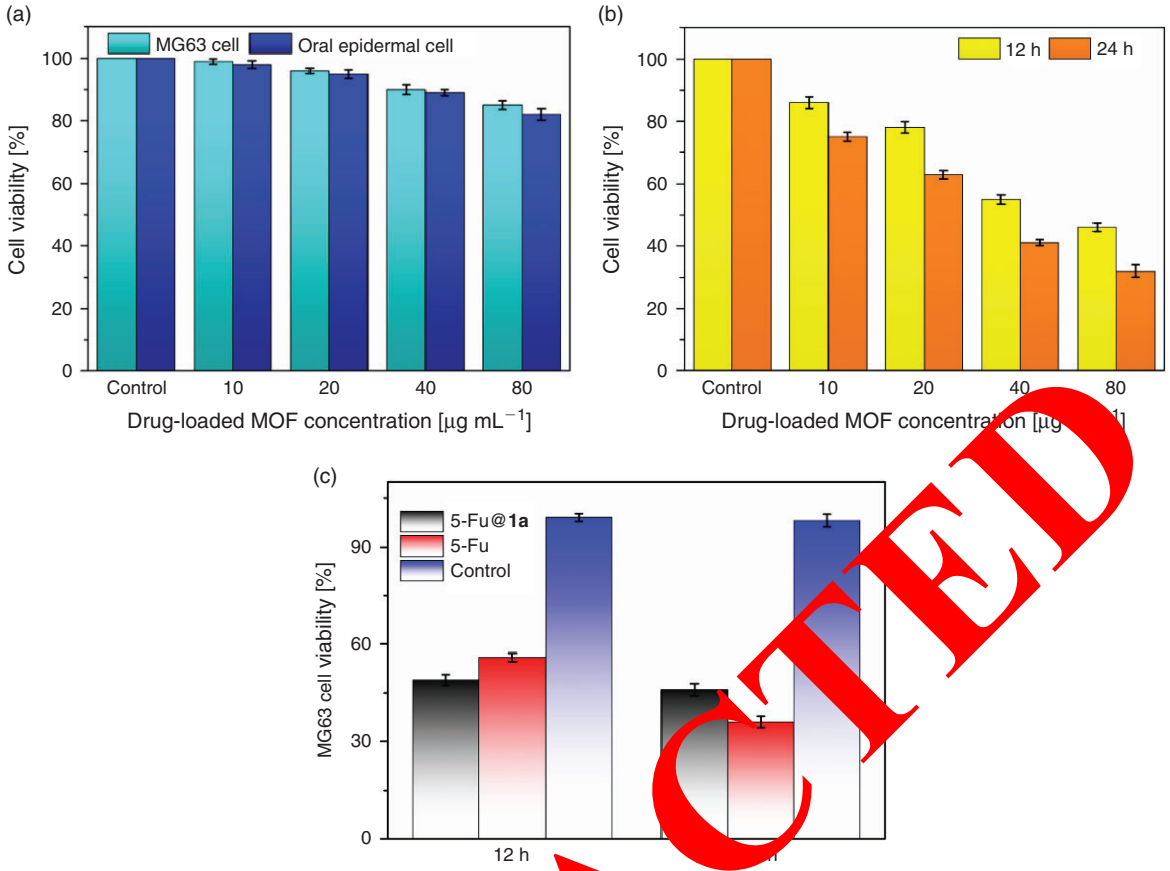

Fig. 5. (a) The viability of human body tumour cells MG63 and oral epidermal cells after exposure to **1a**. (b) Viability of MG63 cells after incubation with various concentrations of drug-loaded MOF at 12 and 24 h. (c) Viability of MG63 cells in the presence of 5-Fu and 5-Fu@**1a** at the 5-Fu concentration of 20 μg mL^{-1}, untreated MG63 cells were considered as a control.

molecules into the solution, resulting in long-lasting 5-Fu release. To obtain the maximum loading as well as the distribution of 5-Fu molecules in the framework of **1a**, the fixed loading task was carried at 37°C and 100 kPa, which reveals that there are eleven 5-Fu molecules in the unit cell of **1a** under the given conditions, corresponding to 22.4 wt-%, which is similar to the value obtained by UV-vis spectroscopy.

Anticancer Activity

To investigate the biocompatibility of **1a** and the potential anticancer activity of 5-Fu@**1a**, the in vitro cell proliferation of **1a** towards MG63 cells (cancer cells) and oral epidermal cells (normal cells) were evaluated via MTT assays. The MG63 cells and the oral epidermal cells were treated with **1a** and the compound concentration was set to four different concentrations (10 to 80 μg mL^{-1} in DMEM). The relationship between the surviving fraction and the drug concentration was plotted to obtain the survival curves. The results show that complex **1** exhibited a negligible cytotoxicity towards the two cell lines tested with more than 80 % of cells alive at the maximum concentration of 80 μg mL^{-1} after 12 and 24 h. These data indicate that our novel drug carrier possesses excellent biocompatibility (Fig. 5a). On the other hand, the drug loaded MOF could lead to significant cell death towards the human bone tumour cells MG63 with an increase of concentration. About 52 % of MG63 cells were killed at 80 μg mL^{-1} of 5-Fu@**1a** in 12 h (Fig. 5b). It should be noted that a further increase of the time to 24 h could result in more cancer cell death, indicating the sustained and prolonged 5-Fu release from **1a**. Furthermore, the efficacy of the 5-Fu and 5-Fu@**1a** were investigated for their ability to eliminate MG63 cells by cell culture experiment. Based on the results in Fig. 5c, the number of living cancer cells in the presence of 5-Fu@**1a** is less than for the free drug 5-Fu, indicating the improved therapeutic effect of loading the 5-Fu into the pores of **1a**.

Conclusion

In summary, by making use of an O-rich organic ligand H_2SDBA, a new 3D porous lanthanide–organic framework with 1D nanosized channels has been synthesised and characterised, which could be used as a pH-sensitive carrier and delivery agent for the anticancer drug 5-Fu. The drug loaded MOF could release more drug molecules at a faster rate in tumour surroundings than in normal physiological conditions. We also characterised the cytotoxicity of 5-Fu@**1a** using an MTT assay towards human body tumour cells MG63, which revealed obvious anticancer activity. The efficient drug loading capacity and progressive release make **1a** a promising carrier for the administration of 5-Fu.

Conflicts of Interest

The authors declare no conflicts of interest.

Acknowledgements

This work was supported by grants from the Medical Science and Technology Research Fund Project of Guangdong Province (B2017050).

References

[1] D. M. Parkin, *Lancet Oncol.* **2001**, *2*, 533. doi:10.1016/S1470-2045(01)00486-7

[2] B. Rosenberg, L. Vancamp, J. E. Trosko, V. H. Mansour, *Nature* **1969**, *222*, 385. doi:10.1038/222385A0

[3] B. Lei, M. Wang, Z. Jiang, W. Qi, R. Su, Z. He, *ACS Appl. Mater. Interfaces* **2018**, *10*, 16698. doi:10.1021/ACSAMI.7B19693

[4] M. Rezaei, A. Abbasi, R. Dinarvand, M. Jeddi-Tehrani, J. Janczak, *ACS Appl. Mater. Interfaces* **2018**, *10*, 17594. doi:10.1021/ACSAMI.8B03111

[5] Y. Feng, H. Fan, Z. Zhong, H. Wang, D. Qiu, *Inorg. Chem.* **2016**, *55*, 11987. doi:10.1021/ACS.INORGCHEM.6B02117

[6] E. K. Ruuge, A. N. Rusetski, *J. Magn. Magn. Mater.* **1993**, *122*, 335. doi:10.1016/0304-8853(93)91104-F

[7] J. Lu, M. Liong, J. I. Zink, F. Tamanoi, *Small* **2007**, *3*, 1341. doi:10.1002/SMLL.200700005

[8] D. Chen, W. Shi, P. Cheng, *Chem. Commun.* **2015**, *51*, 370. doi:10.1039/C4CC07357F

[9] S. K. Mostakim, S. Biswas, *CrystEngComm* **2016**, *18*, 3104. doi:10.1039/C6CE00421K

[10] Y. Feng, M. Li, H. Fan, Q. Huang, D. Qiu, H. Shi, *Dalton Trans.* **2015**, *44*, 894. doi:10.1039/C4DT02840F

[11] M. X. Wu, Y. W. Yang, *Adv. Mater.* **2017**, *29*, 1606134. doi:10.1002/ADMA.201606134

[12] M. Giménez-Marqués, T. Hidalgo, C. Serre, P. Horcajada, *Coord. Chem. Rev.* **2016**, *307*, 342. doi:10.1016/J.CCR.2015.08.008

[13] Y. Bai, Y. Dou, L. H. Xie, W. Rutledge, J. R. Li, H. C. Zhou, *Chem. Soc. Rev.* **2016**, *45*, 2327. doi:10.1039/C5CS00837A

[14] Z. Li, Y. W. Yang, *J. Mater. Chem. B* **2017**, *5*, 9278. doi:10.1039/C7TB02647A

[15] C. He, D. Liu, W. Lin, *Chem. Rev.* **2015**, *115*, 11079. doi:10.1021/ACS.CHEMREV.5B00125

[16] Y. Yang, J. Liu, C. Liang, L. Feng, T. Fu, Z. Dong, Y. Chao, Y. Li, G. Lu, M. Chen, Z. Liu, *ACS Nano* **2016**, *10*, 2774. doi:10.1021/ACSNANO.5B07882

[17] L. L. Tan, N. Song, S. X. A. Zhang, [illegible] Li, [illegible] Wang, Y. W. Yang, *J. Mater. Chem. B* **2016**, *4*, [illegible] doi:10.1039/C5TB01789K

[18] L. L. Tan, H. Li, Y. C. Qiu, D. X. Chen, [illegible] Wang, R. Y. [illegible] Y. Wang, S. X. A. Zhang, B. Wang, Y. [illegible] Yang, *Chem. Sci.* **2015**, *6*, 1640. doi:10.1039/C4SC03749A

[19] I. Abánades Lázaro, S. Haddad, J. M. Rodrigo-Muñoz, C. Orellana-Tavra, V. del Pozo, D. Fairen-Jimenez, R. S. Forgan, *ACS Appl. Mater. Interfaces* **2018**, *10*, 5255. doi:10.1021/ACSAMI.7B17756

[20] Q. L. Li, Y. Sun, L. Ren, X. Wang, C. Wang, L. Li, Y. W. Yang, X. Yu, J. Yu, *ACS Appl. Mater. Interfaces* **2018**, *10*, 29314. doi:10.1021/ACSAMI.8B09330

[21] M. X. Wu, J. Gao, F. Wang, J. Yang, N. Song, X. Jin, P. Mi, J. Tian, J. Luo, F. Liang, Y. W. Yang, *Small* **2018**, *14*, 1704440. doi:10.1002/SMLL.201704440

[22] Y. D. Zhu, S. P. Chen, H. Zhao, Y. Yang, X. Q. Chen, J. Sun, H. S. Fan, X. D. Zhang, *ACS Appl. Mater. Interfaces* **2016**, *8*, 34209. doi:10.1021/ACSAMI.6B11378

[23] P. Horcajada, C. Serre, G. Maurin, N. A. Ramsahye, F. Balas, M. Vallet-Regí, M. Sebban, F. Taulelle, G. Férey, *J. Am. Chem. Soc.* **2008**, *130*, 6774. doi:10.1021/JA710973K

[24] P. Horcajada, C. Serre, M. Vall[illegible]-Regí, M. [illegible]ban, F. Taulelle, G. Férey, *Angew. Chem. Int. Ed.* [illegible]6, *45*, 59[illegible] doi:10.1002/ANIE.200601878

[25] P. Horcajada, R. Gref, T. [illegible]aa[illegible], P. K. A[illegible] G. M[illegible]urin, P. Couvreur, G. Férey, R. E. Morris, C. Serre, *Chem. R[illegible]* **[illegible]012**, *112*, 1232. doi:10.1021/CR200256Y

[26] R. C. Huxford, J. Del[illegible]ca, W. Li, *Curr. Opin. Chem. Biol.* **2010**, *14*, 262. doi:10.1016/J.C[illegible]2009.12.012

[27] K. M. L[illegible]r-Pashow, J. D[illegible]Rocca, Z. Xie, S. Tran, W. Lin, *J. Am. Chem. Soc.* [illegible] *131*, 14261. doi:10.1021/JA906198Y

[28] R. C. Huxford, [illegible] DeKrafft, W. S. Boyle, D. Liu, W. Lin, *Chem. Sci.* **2012**, *3*, 198. doi:[illegible]39/C1SC00499A

[29] M. Bosch, M. Zhang, H. C. Zhou, *Adv. Chem.* **2014**, *2014*, 182327. doi:10.1155/2014/182327

[30] K. Jiang, L. Zhang, Q. Hu, Y. Yang, W. Lin, Y. Cui, Y. Yang, G. Qian, *Mater. Lett.* **2018**, *225*, 142. doi:10.1016/J.MATLET.2018.05.006

[31] [illegible], Q. Hu, Q. Zhang, K. Jiang, W. Lin, Y. Yang, Y. Cui, G. Qian, *Mol. Pharm.* **2016**, *13*, 2782. doi:10.1021/ACS.MOLPHARMACEUT.6B00374

[32] P. F. Gao, L. L. Zheng, L. J. Liang, X. X. Yang, Y. F. Li, C. Z. Huang, *J. Mater. Chem. B* **2013**, *1*, 3202. doi:10.1039/C3TB00026E

[33] A. de Bettencourt-Dias, *Inorg. Chem.* **2005**, *44*, 2734. doi:10.1021/IC048499B

[34] P. Wang, J. P. Ma, Y. B. Dong, R. Q. Huang, *J. Am. Chem. Soc.* **2007**, *129*, 10620. doi:10.1021/JA072442H

[35] Y. Liang, R. Cao, W. Su, M. Hong, W. Zhang, *Angew. Chem.* **2000**, *39*, 3304. doi:10.1002/1521-3773(20000915)39:18<3304::AID-ANIE3304>3.0.CO;2-H